10th ANKARA INTERNATIONAL AEROSPACE CONFERENCE **AIAC-2019-042**
18-20 September 2019 - METU, Ankara TURKEY

A PARAMETRIC COMPARISON OF THE INFLUENCE OF THE WATERJETS ON THE ACOUSTIC PERFORMANCE OF THE SEA VESSELS

Buğra Uğur Yazıcı[1]
STM Savunma Teknolojileri Mühendislik A.Ş.
Istanbul, Turkey

Baha Zafer[2]
Istanbul University-Cerrahpaşa
Istanbul, Turkey

ABSTRACT

Great concern has been raised to emphasize significant amount of the underwater noise generated by human activity related to commercial shipping recently. Rising noise levels that is generated by the human activities can negatively impact ocean life especially for marine mammals in both short and long terms.

International Maritime Organization (IMO) and other bodies have been trying to set-up guidelines in order to reduce noise levels at sea [IMO, 2014]. As clearly stated in mentioned guidelines, for the prediction purposes of the underwater noises, Computational Fluid Dynamics (CFD) methodologies could be applied to predict and visualize flow characteristics related to hull and appendages as well as propellers. Many researches have been undertaken to measure underwater noise originating from propeller rotation. In addition to propellers, hull shape is also crucial for ship-generated noise. Uneven and non-homogeneous wake fields are known to increase cavitation. Therefore; the ship hull form with the appendages should be optimized in the initial phase of the design process to reduce cavitation.

In this paper, parametric study of the vortex control technique based on fluidic actuation for the control of the separated flow from the aft of the vessel will be investigated. Additional water actuator source will be placed at the aft section of the vessel in order to reduce turbulence of the separated flow of the transom. Various length, height and velocity components will be used as the optimization parameters of the underwater noise of the hull form. Hydro-acoustic analysis has been carried out using unsteady Reynolds Averaged Navier Stokes (u-RANS) with Ffowcs-Williams and Hawkings (FWH) model.

INTRODUCTION

The displacement-type ship KRISO Container Ship (KCS) has been chosen to determine the influence of the waterjets on the acoustic performance of the vessel. The KCS was conceived to provide data for both explication of flow physics and CFD validation for a modern container ship with a bulbous bow. Main particulars of the model is given in Table 1. The Korea Research Institute for Ships and Ocean Engineering (KRISO) performed towing tank experiments to obtain resistance, mean flow data and free surface waves [Van et al, 1998(a-b), Kim et al, 2001]. Self propulsion tests were carried out at the Ship Research Institute (now NMRI) in Tokyo and are reported in the Proceedings of the CFD Workshop Tokyo in 2005 [Hino, 2005]. Later, resistance tests were also reported by NMRI [See Zou and Larsson, 2014].

[1] Researcher, Email: bugur.yazici@gmail.com
[2] Assoc.Prof., Email: baha.zafer@istanbul.edu.tr

Data for pitch, heave, and added resistance are available from Force/Dmi measurements reported in Simonsen et al. (2008). Simonsen and Stern (2010) performed CFD RANS simulations to obtain the heave and pitch motions and added resistance for the KCS model, presenting it at the Gothenburg 2010 CFD workshop. In addition, Enger et al. (2010) contributed to the same workshop with their study on the dynamic trim, sinkage and resistance analyses of the KCS model. Recent developments in both numerical modelling methods and increased computational processing capabilities have made it possible to carry out fully non-linear simulations of ship motions, taking into account viscous effects by using CFD tools. Tahsin et al.(2015) made a full-scale analysis of the KCS hull by utilizing aforementioned developments.

Table 1 : Main Particulars of KCS Model

Length Between Perpendiculars (m)	7.2786
Length Waterline (m)	7.3570
Breadth Waterline (m)	1.0190
Depth (m)	0.6013
Draught (m)	0.3418

The ability to predict the amplitude of a sound wave radiated by a solid object in a fluid flow is one of the most significant goals in acoustic field. Lighthill (1952) made an important step in achieving this goal, when he developed a theory, which determines that sound radiated by turbulent flow in a fluid without solid boundaries has quadrupole characteristics. Shortly afterwards, Curle(1955) extended Lighthill’s theory to a flow where immoveable solid objects are present. According to Curle, a sound wave radiated by a flow in the presence of a solid object is the sum of the Lighthill’s quadrupole sound and an acoustic wave generated by the distribution of dipole acoustic sources over the surface of the object. Curle also showed that the strength of the dipole sources is proportional to the total force per unit area on the surface. Curle’s equation can be simplified for an acoustically small object, for which the amplitude of the radiated sound wave is proportional to the total force acting upon the flow from the object. Many practical approaches to the sound radiation problem are based on an equation derived by Ffowcs-Williams and Hawkings (1969). This equation is more general than Curle’s equation and describes flow around a solid object, which moves at an arbitrary speed. Unlike Curle’s equation, Ffowcs Williams and Hawkings (FWH) equation contains a monopole term, which depends on the velocity of the object with respect to a stationary observer. At the same time, the main conlusion of Curle about the dipole characteristics of the radiated sound remains unchanged in the Ffowcs Williams and Hawkings theory, and for an immoveable object the FWH equation reduces to Curle’s equation.

Although abovementioned theories originally developed for the aero-acoustic field, many studies have been carried out for the prediction of marine propeller radiated noise. Seol et al. (2002) investigated the non-cavitating propeller noise employing Boundary Element Methods (BEM) for the calculation offlow around a propeller in timedomain and used FW–H method to predict the far-field acoustics. Salvatore and Ianniello (2003) published the preliminary results for cavitating propeller noise predictions. Ozden et al. (2016) investigated INSEAN E1619 submarine propeller in open water, behind a generic DARPA suboff submarine. For the prediction of the inboard noise level of a three bladed DTMB 4119 model propeller, Tip Vortex Index technique applied by Sezen, S. et. al (2017) coupling an empirical formula with a lifting surface method.

A.Badino et.al (2012) investigated the effect of on board noise radiation for the different type of propulsion systems by comparing the pump-jet and conventional pod. M.F.McKenna et. Al (2012) measured the radiated noise of research vessels by using real-time data with the calibrated acoustic recorders.

NUMERICAL MODELLING

Governing Equations

As suggested by Ferziger and Peric (2002), the averaged continuity and momentum equations may be written in tensor form and Cartesian coordinates for incompressible flows without body forces as follows:

$$\frac{\partial \rho}{\partial t} + \frac{\partial}{\partial x_i}(\rho v_i) = 0 \qquad (1)$$

$$\frac{\partial(\rho v_i)}{\partial t} + \frac{\partial(\rho u_i u_j)}{\partial x_j} = \frac{\partial P}{\partial x_i} + \frac{\partial}{\partial x_j}\left[\mu\left(\frac{\partial u_i}{\partial x_j} + \frac{\partial u_j}{\partial x_i} - \frac{2}{3}\delta_{ij}\frac{\partial u_l}{\partial x_l}\right)\right] + \frac{\partial}{\partial x_j}(-\rho\overline{u_i{}'u_j{}'}) \qquad (2)$$

First equation is the continuity and the second one is the momentum equations where x_i and v_i expresses the tensor form of axial coordinates and velocities, respectively. δ_i is Kronecker Delta, ρ is the density, υ is the kinematic viscosity of the fluid and $-\rho\overline{u_i{}'u_j{}'}$ are the unknown Reynolds stresses.

For the far-field noise predictions, Ffowcs-Williams and Hawking (FWH) method was used. A time domain integral formulation adopted wherein time histories of sound pressure, or acoustic signals, at prescribed receiver locations are directly compute d by evaluating few surface integrals. Time-accurate solutions of the flow field variables, such as pressure, velocity components, and density on source (emission) surfaces, are required to evaluate the surface integrals. Time accurate solutions can be obtained from unsteady Reynolds-averaged Navier–Stokes (URANS) equations, large eddy simulations (LES), or detached eddy simulations (DES). FWH equation is an inhomogeneous wave equation derived from the continuity and Navier–Stokes equations [Ffowcs Williams and Hawkings, 1969 & Brentner and Farassat, 1998].

$$\frac{1}{a_0{}^2}\frac{\partial^2 p'}{\partial t^2} - \nabla^2 p' = \frac{\partial^2}{\partial x_i \partial x_j}\{T_{ij}H(f)\} - \frac{\partial}{\partial t}\{[P_{ij}n_{ij} + \rho u_i(u_n - v_n)]\delta(f)\} + \frac{\partial}{\partial t} \qquad (3)$$
$$\{[\rho_0 v_n + \rho(u_n - v_n)]\delta(f)\}$$

Where p', is the far field sound pressure ($p' = p - p_0$) , T_{ij} is the Lighthill tensor and a_0 is the sound velocity in the far field. The terms at RHS are defined as quadruple, dipole and monopole source, respectively. Also $\delta(f)$ is the Dirac delta function and $H(f)$ is the Heaviside function.

Physics Modelling

The turbulence model selected in this study was a standard k–ε model, which has been extensively used for industrial applications (CD-Adapco, 2018). Also, Querard et al. (2008)note that the k–ε model is quite economical in terms of CPU time, compared to, for example, the SST turbulence model, which increases the required CPU time by nearly 25%.

The“Volume of Fluid” (VOF) method was used to model and position the free surface. CD-Adapco (2018) defines the VOF method as,“a simple multiphase model that is well suited to simulating flows of several immiscible fluids on numerical grids capable of resolving the interface between the mixture's phases”. Because it demonstrates high numerical efficiency, this model is suitable for simulating flows in which each phase forms a large structure, with a low overall contact area between the different phases.

The inlet velocity and the volume fraction of both phases in each cell, as well as the outlet pressure are all functions of the flat wave used to simulate the free surface. The free surface is not fixed, it is dependent on the specifications with the VOF model making calculations for both the water and air phases. The grid is simply refined in accordance with ITTC (2011b) in order to enable the variations in volume fraction to be more accurately captured. In this work, a second-order convection scheme was used throughout all simulations in order to accurately capture sharp interfaces between the phases. Convection terms in the RANS formulae were discretized by applying a second-order upwind scheme. The overall solution procedure was obtained according to a SIMPLE-type algorithm. In order to simulate realistic ship behavior, a Dynamic Fluid Body Interaction (DFBI) model was used with the vessel free to move in the pitch (rotational movement around x axis) and heave (directional movement in z direction). The DFBI model enabled the RANS solver to calculate the exciting force and moments acting on the ship hull due to waves, and to solve the governing equations of rigid body motion in order to re-position the rigid body [CD-Adapco, 2018].

“Farassat_1A” formulation of Ffowcs-Williams Hawkings method was used to predict radiated noise levels. CD-Adapco (2018) defines the formulation as “Farassat’s Formulation 1A is the default and preferred formulation, a non-convective form of FW-H for general subsonic source regions, including the Impermeable formulation for transient rotating motion, in both whole and periodic domains.” The FW-H equation is an exact rearrangement of the continuity and the momentum equations into the form of an inhomogeneous wave equation. The FW-H equation gives accurate results even if the surface of integration lies in the nonlinear flow region. It is based on the free-space Green’s function to compute the sound pressure at the observer location which should be determined before the analysis starts. When aforementioned integral function is calculated, integration surface of the mesh structure coincides with the surface of the solid body, CD-Adapco (2018) defines three solution terms; the monopole term, the dipole term and the quadrupole.

Boundary Conditions

Boundary conditions of the inlet surfaces and outlet surfaces have been selected as Velocity-Inlet and Pressure-outlet respectively. Side surface and cut plane have been selected as symmetry plane. Boundary condition for top and bottom surfaces are the same as inlet surface. Hull surfaces have been selected as wall condition. Boundary conditions for the solution domain and hull are shown in Figure 1.

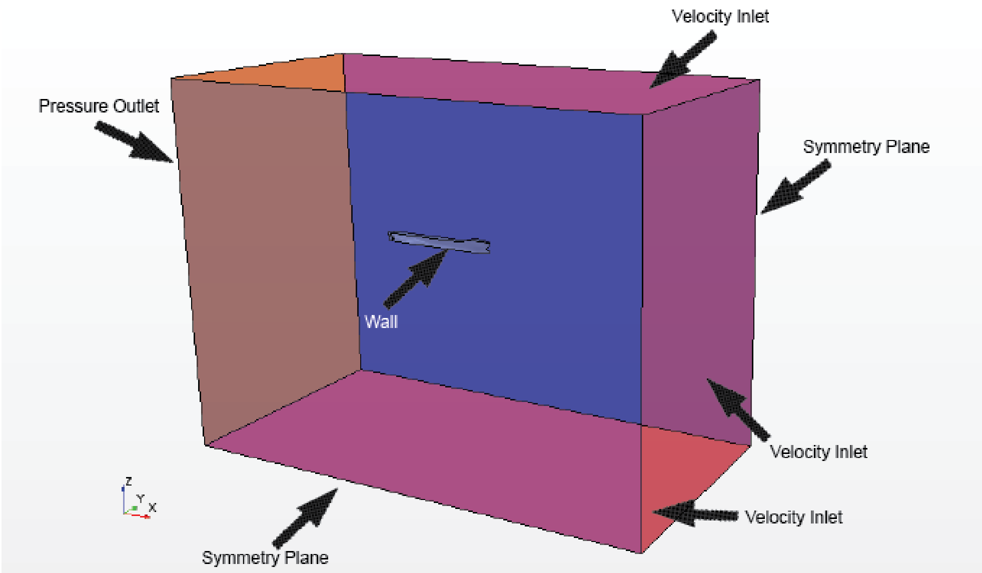

Figure 1: Boundary Conditions for the Mesh

Mesh Generation

Mesh generation was performed using the automatic meshing facility in STAR-CCM+, which uses the Cartesian cut-cell method. Final mesh which is shown in Figure 2 is resulted in a computation mesh of 1016776 cells. A trimmed cell mesher was employed to produce a high-quality grid for complex mesh generating problems.

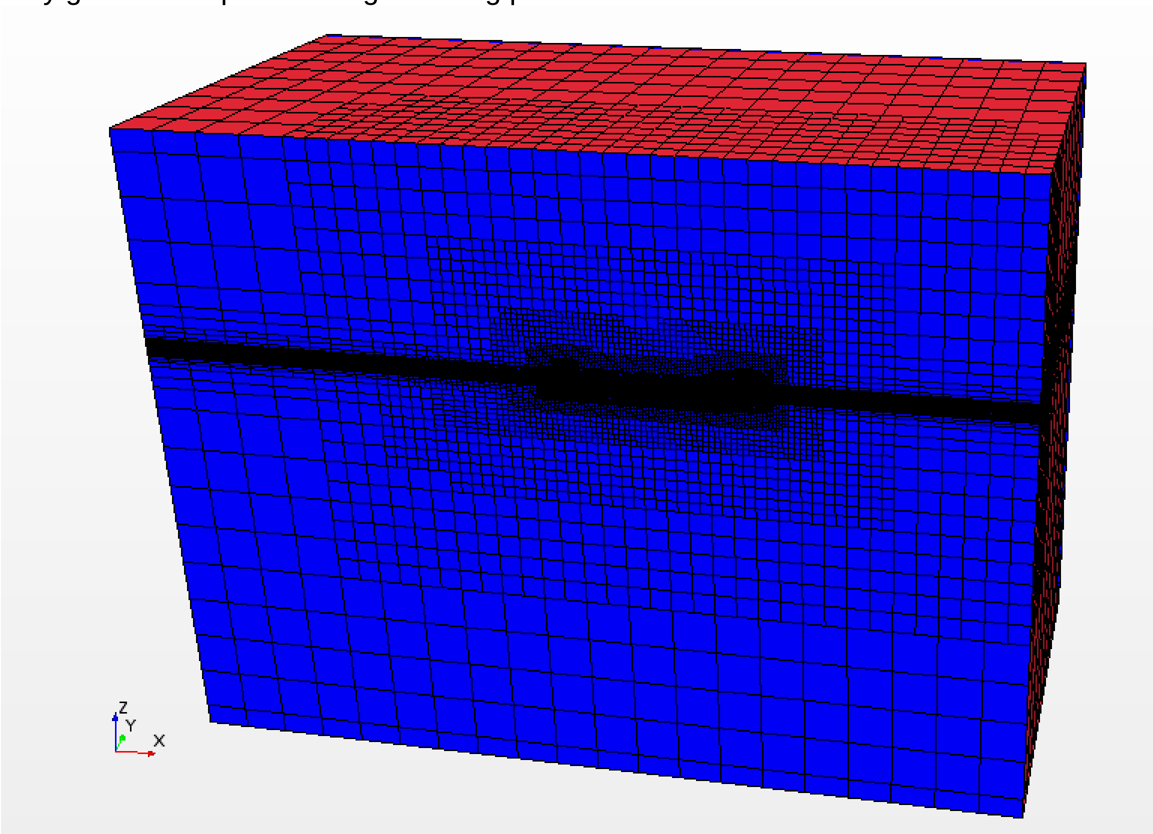

Figure 2: Cartesian Mesh of the Domain

In order to have better results in the near field of wall surfaces, total number of six prism layers are implemented with the 1.5 expansion rate. Mesh sizes have been optimized within the well known Kelvin wake pattern area whis is shown in Figure 3 from the bow of the ship to the aft section.

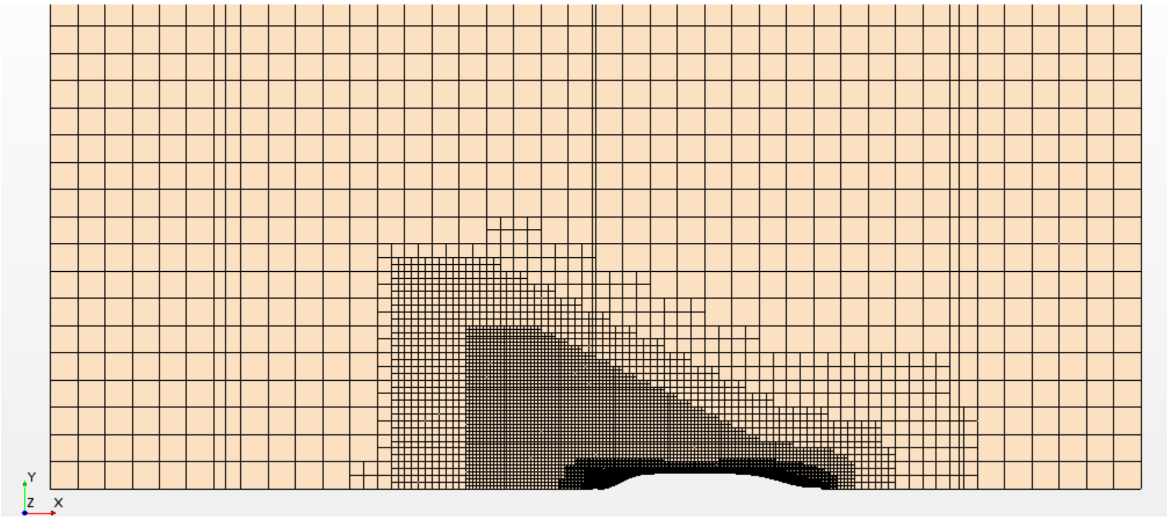

Figure 3: Mesh Refinement within the Kelvin Wake Pattern

VALIDATION

For the validation of the CFD calculations, experimental data for the resistance values which is available at KRISO (Korea) and SRI (Japan) has been compared to the obtained data. Test condition of the validation case is given in Table 2.

Table 2 : Test Data of KCS Model

U (m/s)	2.196
Fn (based on Lpp)	0.26

After verification study, result of the CFD analysis has been validated with the experimental result. Y+ values have been checked on the hull surface and found maximum of 287.6 (Figure 4) which shows results are acceptable with the turbulence model. Total resistance force for half body simulation has been found as 39.96N. The comparison between CFD analysis and the experiment data [Fujisava et al., 2000] are shown in Table 4.

Table 3 : CFD and Experimental Results

CFD					Experiment		
Half Body Resistance (N)	WSA (m2)	Sinkage	Trim	C_{Tm}	Sinkage	Trim	C_{Tm}
42.056	4.821	-1.40E-02	-1.56E-01	3.66E-03	-1.39E-02	-1.69E-01	3.53E-03

Table 4 : Comparison between CFD and Experimental Results

Relative Error		
Sinkage	Trim	C_{Tm}
0.50%	-8.66%	0.33%

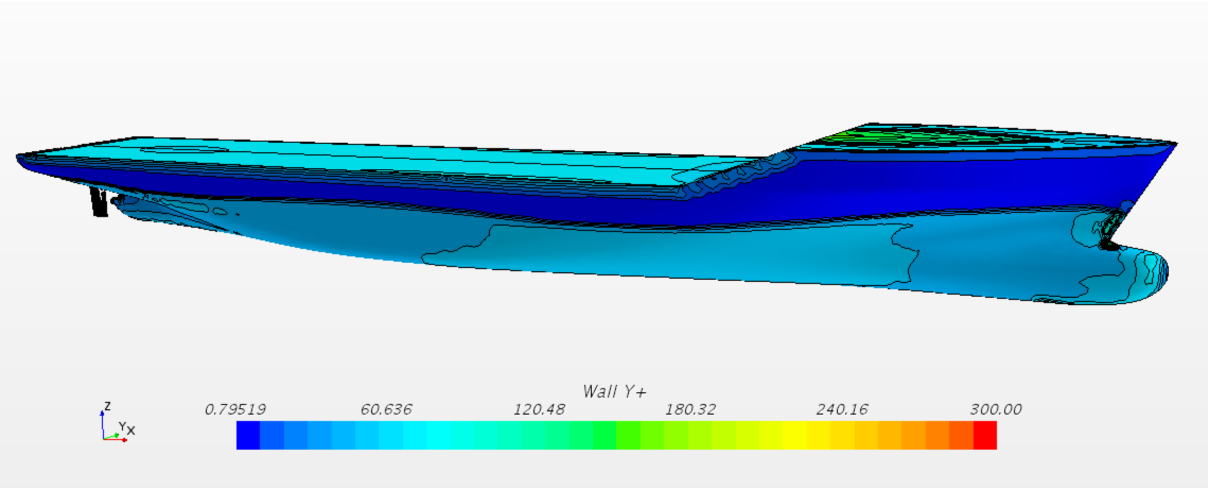

Figure 4: Wall y-plus Values

WATERJET NOISE ANALYSIS

In order to evaluate the waterjet effect on the ship hull, three locations behind the hull were selected. In Figure 5, waterjet area and the middle point of the same areas from the base and centerline of the model are shown in model scale. As distinct from the above analysis, waterjet areas are split from the hull geometry by making their boundary conditions velocity inlet with the direction of –x vector (-1, 0, 0).

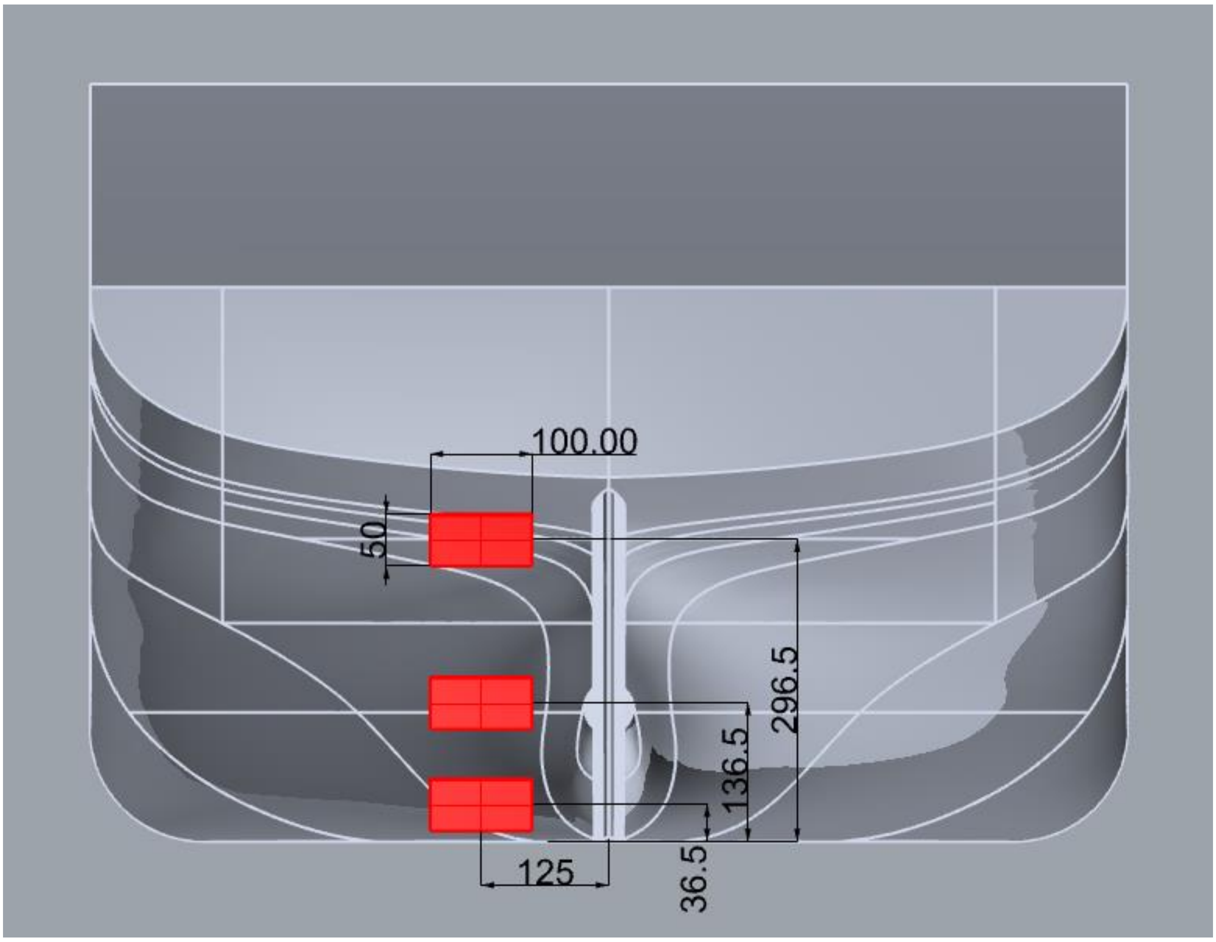

Figure 5: Water Jet Locations on the Model Scale (Looking from aft)

In addition to the three waterjet locations, two waterjet velocity that are equal to model hull speed and half of the model hull speed are chosen to investigate whether speed of the jet has effect on the noise. Totally 6 cases were investigated as shown in Table 5.

Table 5 : Waterjet Analysis Cases

Cases	Jet Location	Jet Speed
Case 1	Upper Jet in Figure 5	U_{model} / 2
Case 2	Upper Jet in Figure 5	U_{model}
Case 3	Middle Jet in Figure 5	U_{model} / 2
Case 4	Middle Jet in Figure 5	U_{model}
Case 5	Lower Jet in Figure 5	U_{model} / 2
Case 6	Lower Jet in Figure 5	U_{model}

6 hydrophones were selected and located 0.5 and 1 meters away from the center of the stern tube where propeller is located on the model. Hydrophones are directed to the direction of aft, port side and the bottom of the model. Locations of the hydrophones are shown in Figure 6 and detailed explanation of the abbreviations for the result plots are shown in Table 6.

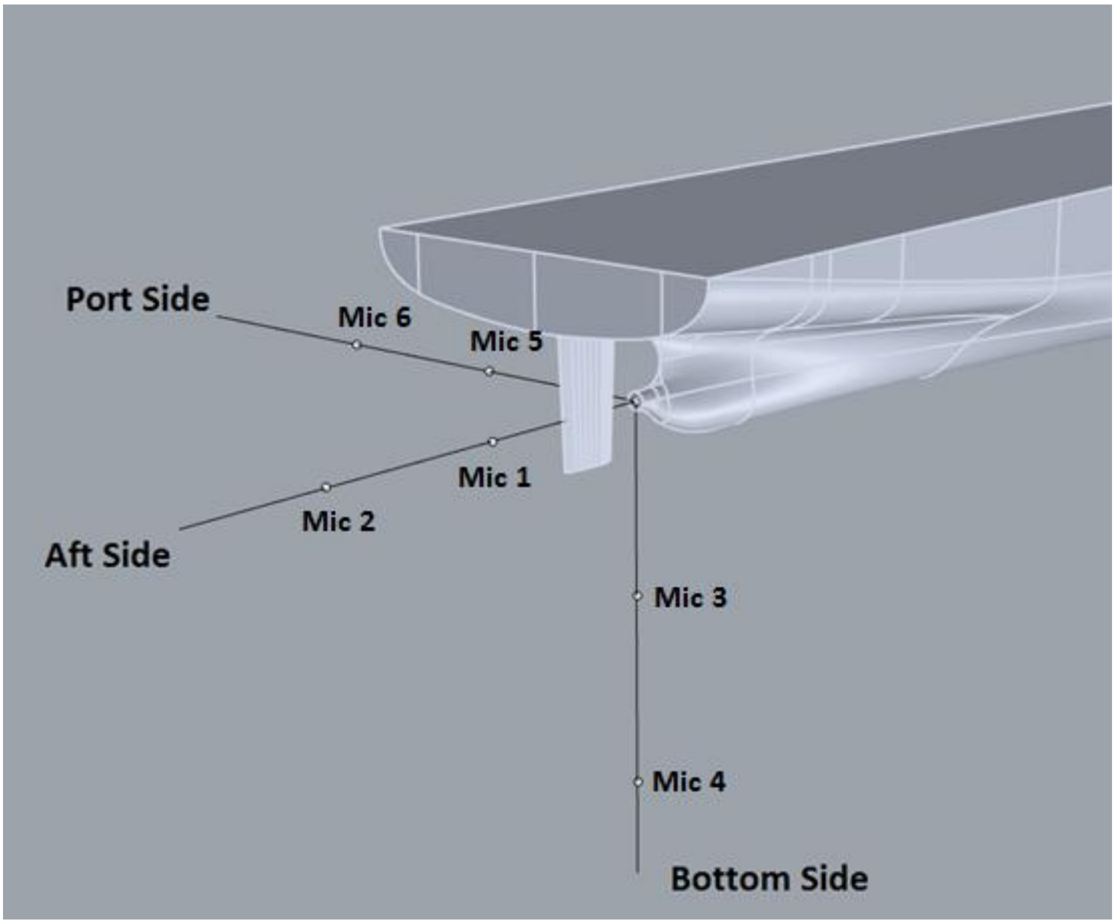

Figure 6: Hydrophones on the Model Scale

Table 6: Hydrophone Abbreviations and Explanations

Abbreviation	**Explanation**
Mic 1	Hydrophone located on the back (-x) side of the center and 0.5 meters away from center
Mic 2	Hydrophone located on the back (-x) side of the center and 1 meters away from center
Mic 3	Hydrophone located on the bottom (-z) side of the center and 0.5 meters away from center
Mic 4	Hydrophone located on the bottom (-z) side of the center and 1 meters away from center
Mic 5	Hydrophone located on the left (y) side of the center and 0.5 meters away from center
Mic 6	Hydrophone located on the left (y) side of the center and 1 meters away from center

RESULTS

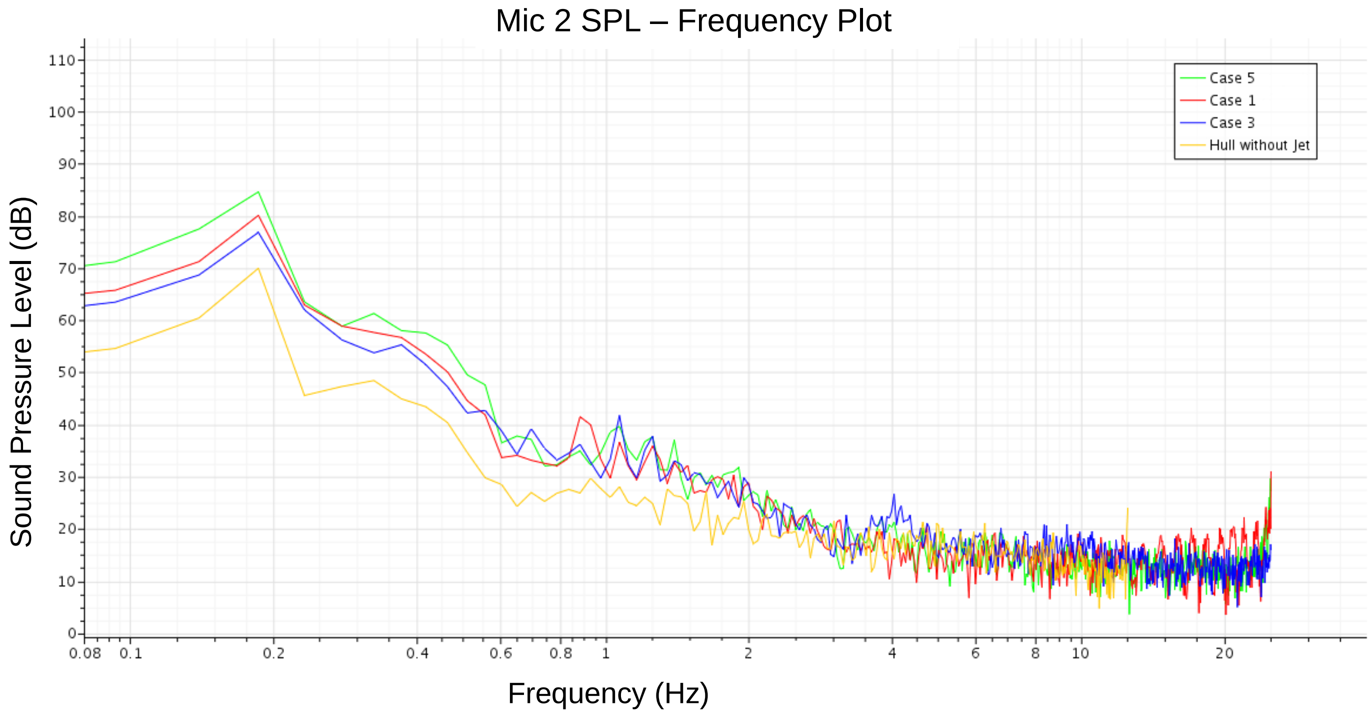

Figure 7.a: Sound Pressure Level Plot of Case Mic 2 for Half Jet Velocities

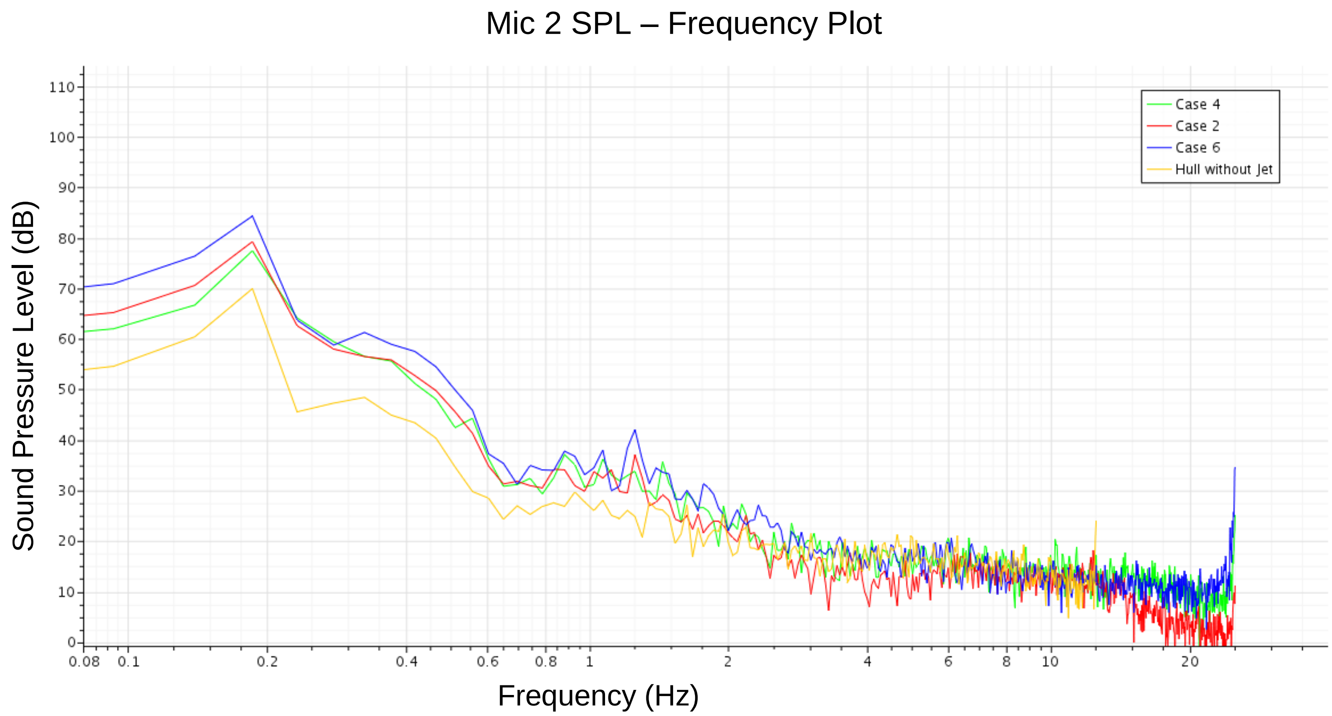

Figure 7.b: Sound Pressure Level Plot of Case Mic 2 for the Same Jet Velocities

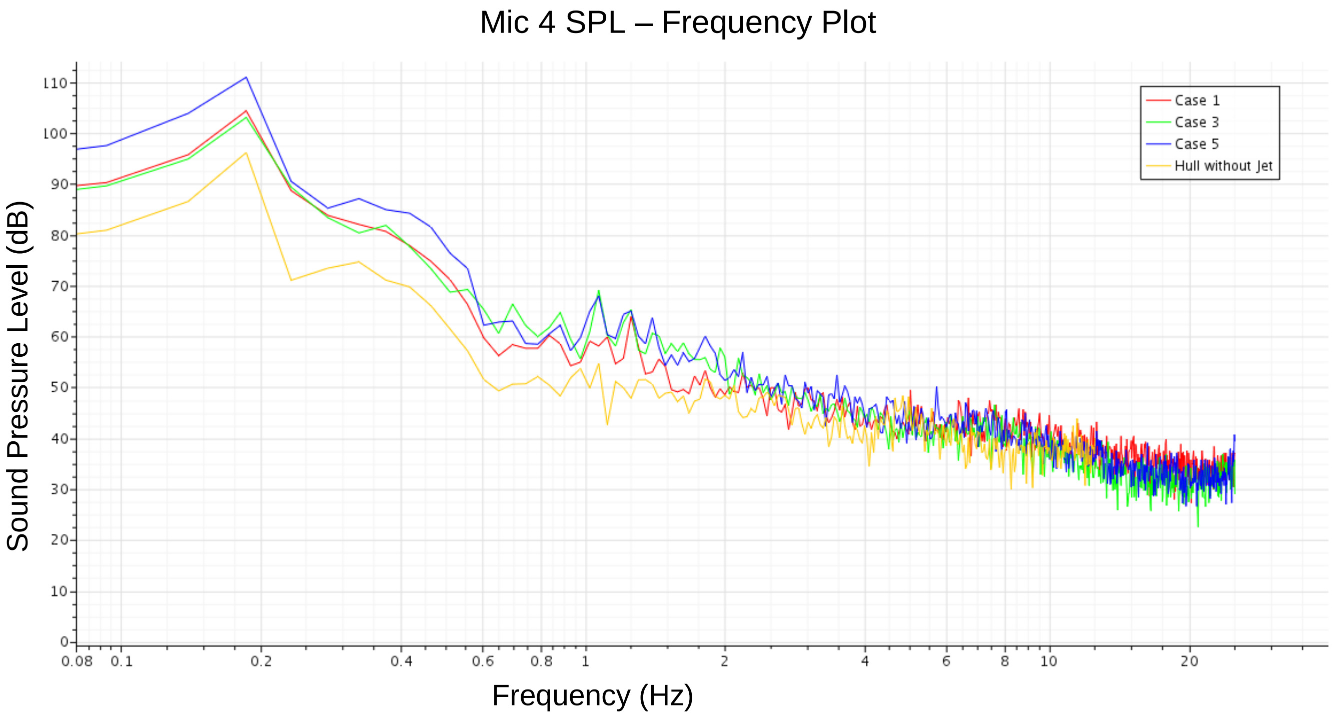

Figure 8.a: Sound Pressure Level Plot of Case Mic 4 for Half Jet Velocities

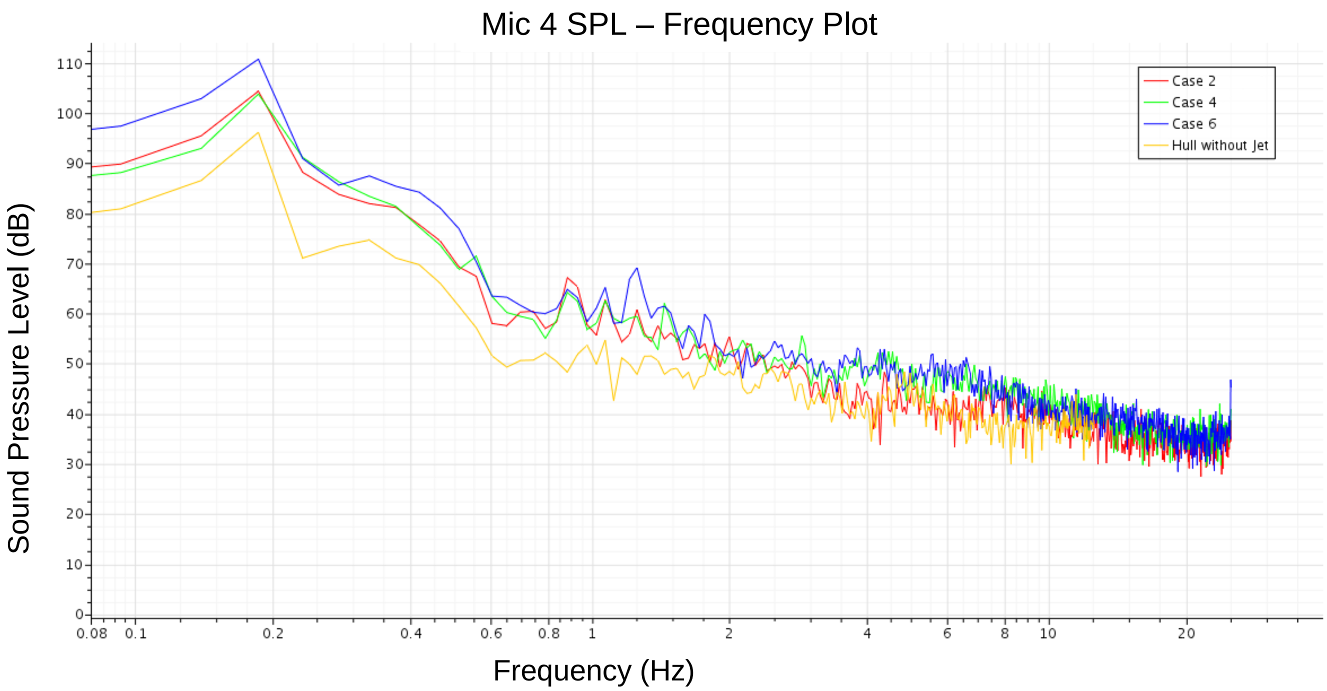

Figure 8.b: Sound Pressure Level Plot of Case Mic 4 for the Same Jet Velocities

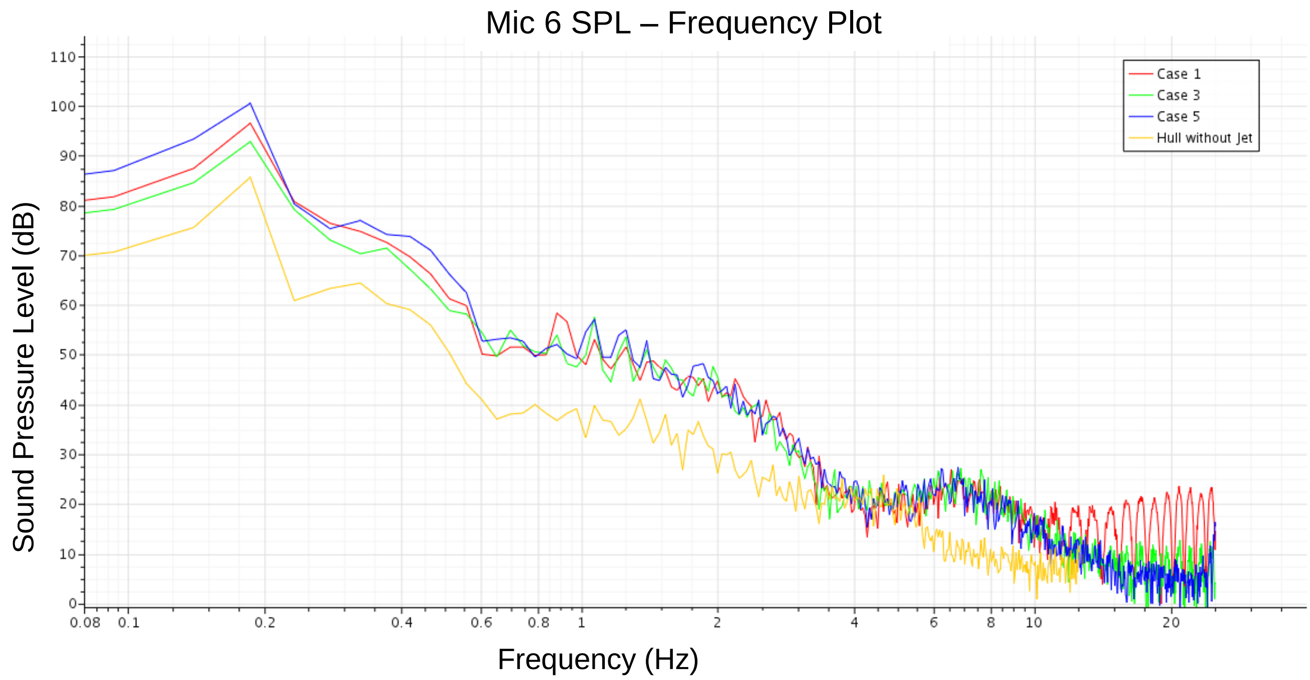

Figure 9.a: Sound Pressure Level Plot of Case Mic 6 for Half Jet Velocities

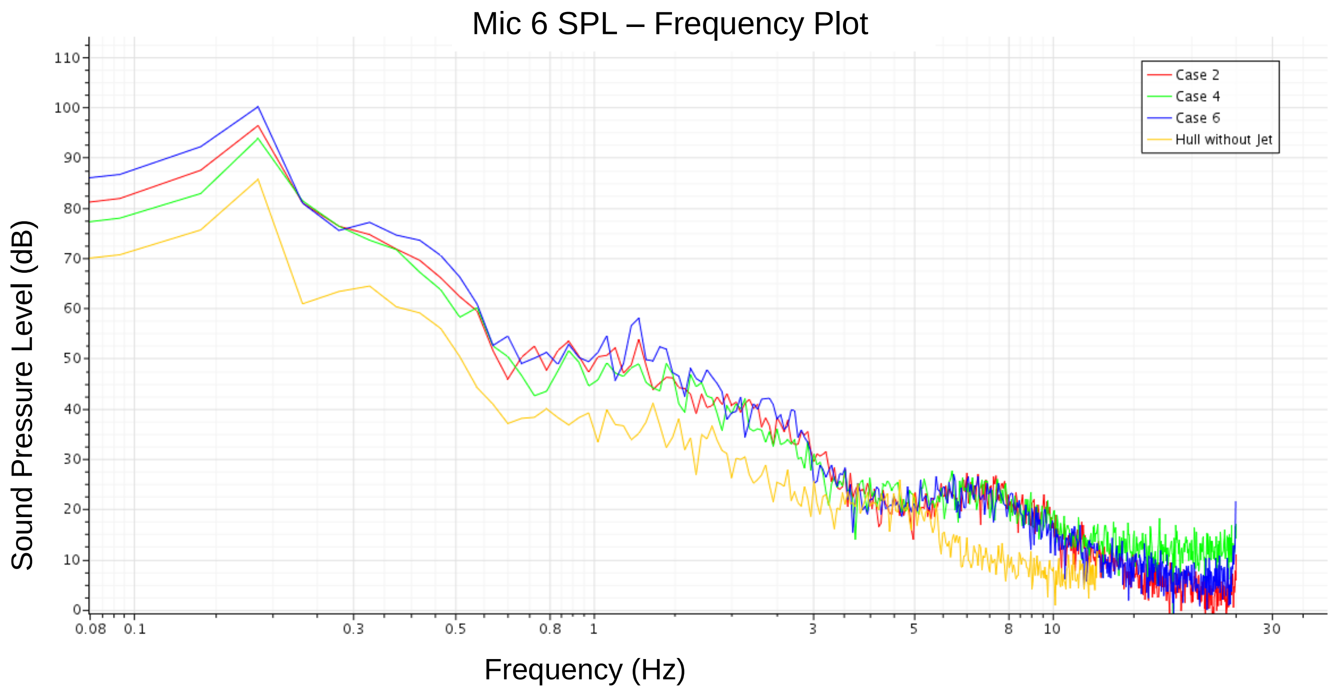

Figure 9.b: Sound Pressure Level Plot of Case Mic 6 for the Same Jet Velocities

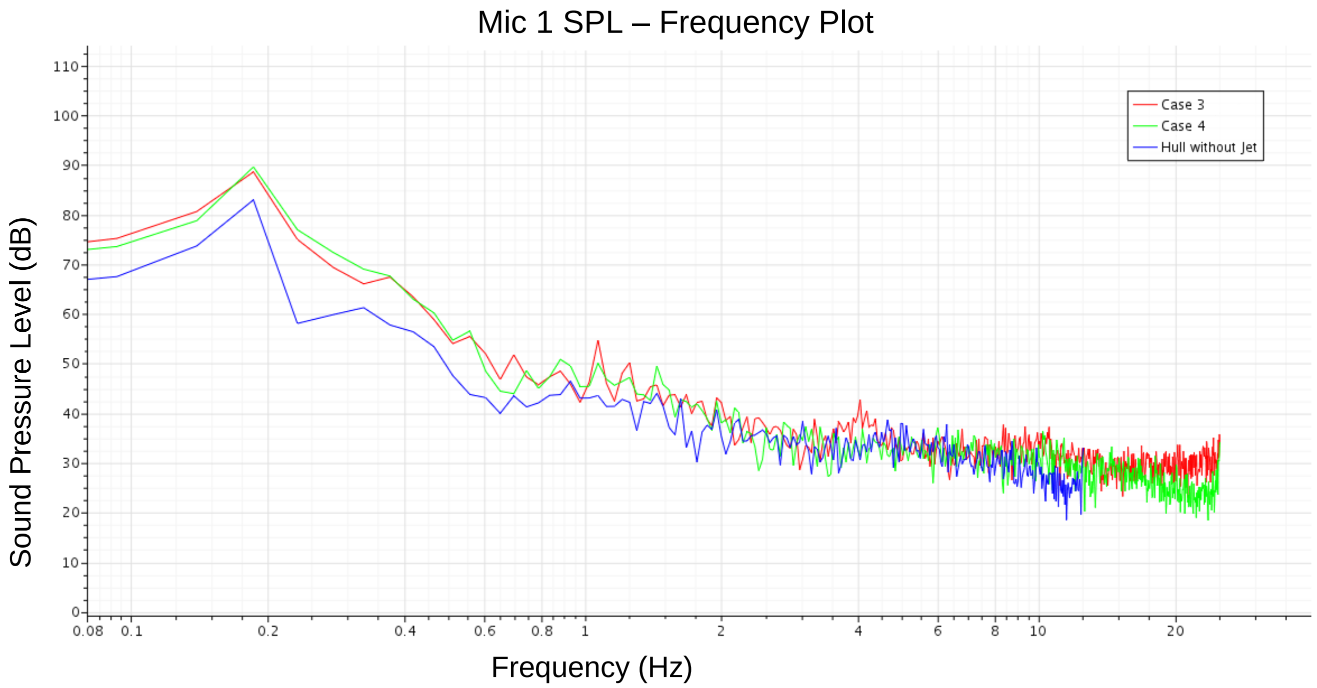

Figure 10.a : Sound Pressure Level Plot of Mic 1 for Middle Jet Cases

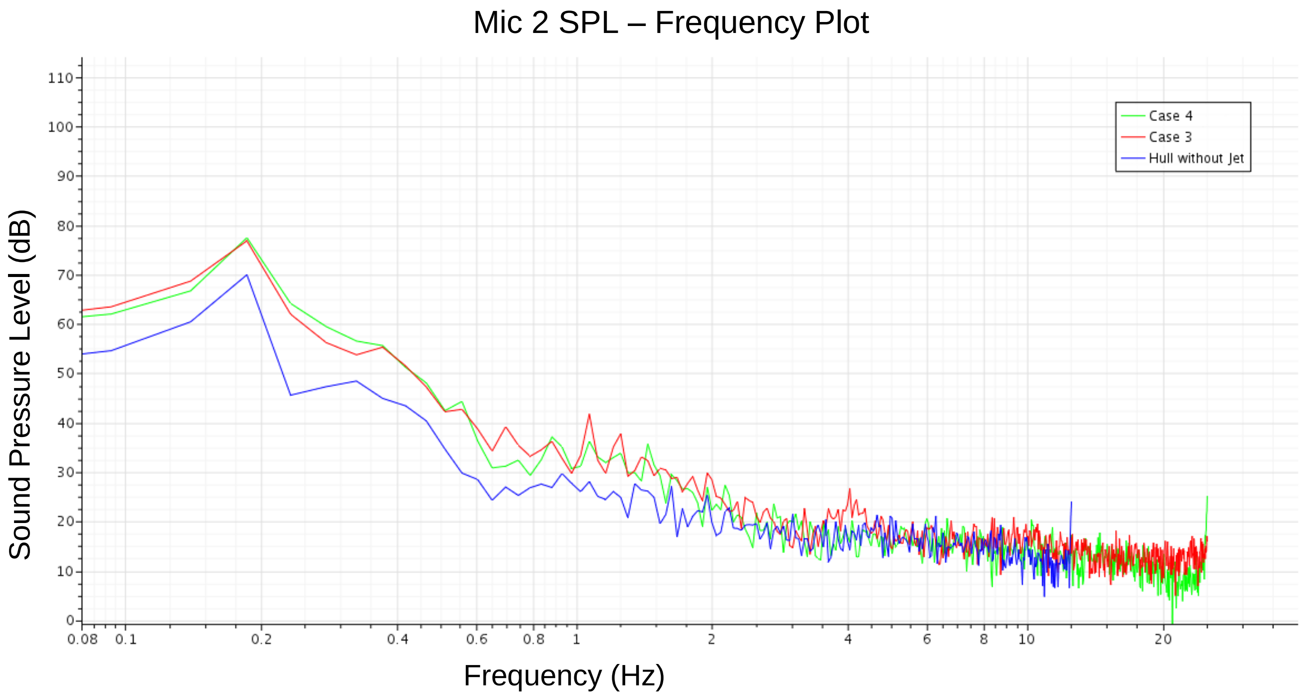

Figure 10.b : Sound Pressure Level Plot of Mic 2 for Middle Jet Cases

A common practice in the analysis and presentation of the noise levels is to reduce the measured or computed values of Sound Pressure Levels (SPL) in each 1/3 Octave band to an equivalent 1 Hz bandwidth by means of the correction formula recommended by ITTC (2008) as follows:

$$SPL_1 = SPL_m - 10 \log \Delta f \tag{4}$$

where SPL_1 is the reduced sound pressure level to 1 Hz bandwidth in dB; re 1μPa (standard reference pressure for water), SPL_m is the measured or computed sound pressure level at each centre frequency in dB; re 1μPa and Δf is the bandwidth for each one-third octave band filter in Hz. The ITTC also required that the sound pressure levels be corrected to a standard measuring distance of 1 m using the following relationship:

$$SPL = SPL_1 + 20 \log(r) \tag{5}$$

where SPL is the equivalent 1 Hz at 1 m distance sound pressure level (in dB; re 1μPa) and r is the vertical reference distance for which thenoise level is measured or receiver locations from the propeller. Hanning filter was used and results were graphically presented where; the logarithmic-scaled x-axis represents the centre frequencies in Hz, while the linear-scaledy-axis represents the sound pressure levels in dB re 1μ, 1 Hz, 1 m, for all cases presented in this paper.

Table 7: Acoustic and Hydrodynamic Analysis Results and Comparison

	SPL (dB)						DRAG			BODY TRANSLATION	
	Mic 1	Mic 2	Mic 3	Mic 4	Mic 5	Mic 6	Pressure (N)	Shear (N)	Total (N)	Sinkage (m)	Trim (deg)
Case 1	99.821	87.749	104.052	112.070	104.052	103.436	2.440	31.534	34.197	-0.016	0.146
Case 2	98.354	85.492	102.349	112.223	102.349	100.873	1.344	31.811	33.376	-0.016	0.135
Case 3	97.716	84.585	100.963	110.705	110.329	99.418	-2.173	31.460	29.287	-0.016	0.177
Case 4	99.079	86.161	103.392	113.057	112.547	101.945	-1.179	31.849	30.669	-0.015	0.154
Case 5		91.644	108.428	117.966	118.026	107.127	1.950	31.426	33.376	-0.018	0.039
Case 6	98.659	85.705	102.200	111.745	111.401	100.732	-2.487	31.855	29.604	-0.018	0.025
Hull with Rudder		72.488	88.29531	98.8826	97.6164	86.769	10.61	31.52	42.126	-0.014	0.156

EVALUATION / CONCLUSION

As it can be seen in Table 7, shear force-induced drag values are decreased in Case 3 and Case 5 compared to the case where no water jet was used. The total drag values are dramatically reduced at least 15% depending on the addition of water jet linked to the pressure drag values. Sinkage values were also decreased. In addition to mentioned effects, dramatic changes of ship trim values for Case 5 ve Case 6 are obtained but other two cases mildly change is noted such as Case 1 and Case 2.

However, despite all these hydrodynamic changes, hydroacoustic values did not decrease. There is even an increase of 10 dB to the environment. As a result of this general evaluation, in new studies, where 0.3 and 0.1 U_{model} velocities instead of 0.5 U_{model} jet velocity and jet angle is less than 90 degrees will be restudied for both hydrodynamic and hydroacoustic changes.

References

A.Badino, D.Borelli, T.Gaggero, E.Rizzuto. (2012) *Criteria for noise annoyance evaluation on board ships. Sustainable Maritime Transportation and Exploitation of Sea Resources*.

CD-Adapco,(2018) *User guide STAR-CCM+ Version 13.06.012.*

Enger, S., Peric, M., Peric, R. (2010) *Simulation of flow around KCS-hull. In: Proceedings from Gothenburg 2010—A Workshop on Numerical Ship Hydrodynamics, Gothenburg*.

Farassat, F., Myers, M.K. (1998) *Extension of Kirchhoff's formula to radiation from moving surfaces. J. Sound Vib. 123 (3), 451–460.*

Fujisawa, J., Ukon, Y., Kume, K., and Takeshi, H. (2000) *"Local Velocity Field Measurements around the KCS Model (SRI M.S.No.631) in the SRI 400m Towing Tank"* Ship Performance Division Report No. 00-003-02, The Ship Research Institute of Japan.

Hino, T. (2005), *"Proceedings of CFD Workshop Tokyo 2005"*, NMRI report.

IMO MEPC.1/Circ.833. (2014) *Guidelines for the Reduction of Underwater Noise from Commercial Shipping to Address Adverse Impacts on Marine Life.*

J.E.Ffowcs Williams and D.L. Hawkings . (1969) *Sound generation by turbulence and surfaces in arbitrary motion, Phil. Trans. Roy. Soc. (London) Ser. A, 264, 321 – 342.*

Kim, W.J., Van, D.H. and Kim, D.H. (2001) *"Measurement of flows around modern commercial ship models", Exp. in Fluids, Vol. 31, pp 567-578.*

M. F. McKenna, D.Ross.(2012) *Underwater radiated noise from modern commercial ships, Acoustical Society of America.*

M.C. Ozden, A. Y.Gürkan, Y.A. Ozden, T.G.Canyurt, E. Korkut. (2016) *Underwater radiated noise prediction for a submarine propeller in different flow conditions*, Ocean Engineering Volume 126, Pages 488-500.

M.J.Lighthill (1952), *On sound generated aerodynamically*, Proc. Roy. Soc. A, 211, 564 – 586.

N.Curle (1955), *The influence of solid boundaries upon aerodynamic sound*, Proc. Roy. Soc. A 231, 505 – 514.

Salvatore, F., Ianniello, S. (2003), *Preliminary results on acoustic modelling of cavitating propellers.* Comput. Mech. 32, 291–300.

Seol, H., Suh, J.C., Lee, S (2002), *Prediction of non-cavitating underwater propeller noise*. J. Sound Vib. 257 (1), 131–156.

Simonsen C.D., Stern, F. (2010), *CFD simulation of KCS sailing in regular head waves.* In: Proceedings from Gothenburg 2010—A Workshop on Numerical Ship Hydrodynamics, Gothenburg.

Simonsen, C., Otzen, J., and Stern, F. (2008), “EFD and CFD for KCS heaving and pitching in regular head waves,” Proc. 27th Symp. Naval Hydrodynamics, Seoul, Korea.

Tsukada, Y., Hori, T., Ukon, Y., Kume, K., and Takeshi, H. (2000), *"Surface Pressure Measurements on the KCS Model (SRI M.S.No.631) in the SRI 400m Towing Tank"* Ship Performance Division Report No. 00-004-01, The Ship Research Institute of Japan.

Van, S.H., Kim, W.J., Yim, G.T., Kim, D.H., and Lee, C.J. (1998), *"Experimental Investigation of the Flow Characteristics Around Practical Hull Forms"* Proceedings 3rd Osaka Colloquium on Advanced CFD Applications to Ship Flow and Hull Form Design, Osaka, Japan.

Zou, L. and Larsson, L. (2010), “Additional data for resistance, sinkage and trim”, in Larsson et al.: "Numerical Ship Hydrodynamics - An Assessment of the Gothenburg 2010 Workshop", Springer Business Media, Doordrecht.